ELSEVIER

Journal of Nuclear Materials 270 (1999) 221–232

journal of nuclear materials

Prediction of the oxygen potential in the fuel-to-clad gap of defective fuel rods during severe accident conditions

B.J. Lewis *

Department of Chemistry and Chemical Engineering, Royal Military College of Canada, P.O. Box 17000 Stn Forces, Kingston, Ont., Canada K7K 7B4

Received 29 April 1998; accepted 22 September 1998

Abstract

A model has been developed to describe the multi-component transport of steam, hydrogen and stable fission-product gas in the fuel-to-clad gap of defective fuel rods during severe reactor accident conditions. The incoming steam must diffuse into the breached rod against any counter-current flow of non-condensable fission gases and out-flowing hydrogen that is produced from the internal reaction of the steam with the Zircaloy cladding or urania. This treatment is used to predict the local molar distribution of hydrogen and steam so that the internal oxygen potential can be estimated along the gap as a function of time. The oxygen potential will directly influence the fuel oxidation state and the fission product release characteristics. The model also considers the effects of mass transfer and changing boundary conditions at the defect site, as steam in the reactor coolant system flows over the defective rod and reacts with the external cladding surface.

1. Introduction

In a fuel rod with a cladding defect, the volatile fission-product gases that are released from the fuel matrix will migrate along the fuel-to-clad gap toward the defect site, and eventually into the reactor coolant system (RCS). The transport of the short-lived volatile fission products in the gap has been studied extensively during normal reactor operation. [1–7] In the absence of any pressure fluctuations in the RCS, diffusion is shown to be the dominant process of transport in the gap. [8,9] During a reactor transient, the presence of higher fuel temperatures and the possible occurrence of steam-oxidation of the uranium dioxide fuel following clad rupture may lead to enhanced and continuous stable gas release from the fuel matrix. If, in addition, the RCS pressure is reduced as a result of coolant blowdown, a pressure differential may result between the internal void volume of the defective rod and the RCS pressure, leading to a bulk-flow contribution [8–10].

Thus, for transient conditions, an enhanced fission-gas release into the fuel-to-clad gap may result. In high-temperature steam, the cladding will remain in place as it is converted to zirconium dioxide. However, for fuel oxidation to take place, steam must diffuse into the breached element against any counter-current flow of non-condensable fission gases, and out-flowing hydrogen that is produced from internal reaction of the incoming steam with the Zircaloy cladding or urania. The molar flux of a given gaseous component in the gap will be derived from both a diffusive flux and total molar bulk flow. Consequently, it is important to determine the molar concentration distribution along the gap for the multi-component (steam, hydrogen and fission gas) mixture since the oxygen potential (i.e., oxygen partial pressure) in the gap will depend on the local constituent partial pressures. The oxygen potential, in turn, will directly affect the fuel oxidation state, and hence the rate of fission-product diffusion in the fuel matrix and the subsequent release into the gap [11]. In addition, the oxygen potential will dictate the amount of fuel volatilization, as well as the chemical form of the fission product [12–14]. The chemical speciation will determine the amount of vaporization of low-volatile products

* Corresponding author. Tel.: +1-613 541 6611; fax: +1-613 542 9489; e-mail: lewis_b@rmc.ca.

0022-3115/99/$ – see front matter
PII: S0022-3115(98)00770-3

from the fuel surface [12,13]. For instance, the fission product release kinetics were observed to differ in annealing experiments conducted at high temperature in steam with bare fuel fragments versus mini-elements (i.e., short-length Zircaloy-clad fuel specimens), even after the clad had been completely oxidized [15,16]. This observation can be attributable to a reduced transport in the gap and a lower oxygen potential as a result of inhibited steam penetration into the mini-elements.

In previous work, the effect of a reduced oxygen potential in the gap was modelled by simply reducing the given oxygen potential in the bulk coolant by an empirical factor; i.e., this factor was derived by matching the predicted fuel oxidation kinetics to the observed end-state weight gain for a mini-element in a specific annealing experiment [11]. In contrast, in the present analysis, a complete mathematical model is developed for multi-component transport in the fuel-to-clad gap of a breached fuel rod. A methodology for the solution of the time-dependent steam, hydrogen and fission gas distributions in the fuel-to-clad gap is given. With a knowledge of the molar distributions, the oxygen potential can be directly estimated. This model also accounts for the resultant hydrogen/steam distribution in the reactor coolant system (i.e., at the defect site) as a result of hydrogen production from external Zircaloy-clad oxidation, as well as the effect of steam reaction in the gap with the internal Zircaloy surface and urania fuel.

2. Model development

2.1. Gap transport equations

The transport equations for the one-dimensional multi-component flow of steam, hydrogen and stable fission gases in the thin, annular, fuel-to-sheath gap (see Fig. 1) follows from the standard conservation expression [17]

$$\frac{\partial c_i}{\partial t} = -\frac{\partial N_i}{\partial z} + q_i - r_i. \tag{1}$$

Here for a given component i, c_i (mol m^{-3}) is the molar concentration, N_i is the molar flux in the z-direction (mol m^{-2} s^{-1}) (resulting from diffusion and a total bulk molar flow), and q_i and r_i are the production and loss rates, respectively (in mol m^{-3} s^{-1}). The fluxes and concentration gradients in an ideal gas mixture of n components are related by the Stefan–Maxwell equations [17]

$$\frac{\partial y_i}{\partial z} = \sum_{j=1, j\neq i}^{n} \frac{1}{cD_{ij}} \left[y_i N_j - y_j N_i \right], \tag{2}$$

where c is the total molar concentration

$$c = \sum_{j=1}^{n} c_j \tag{3}$$

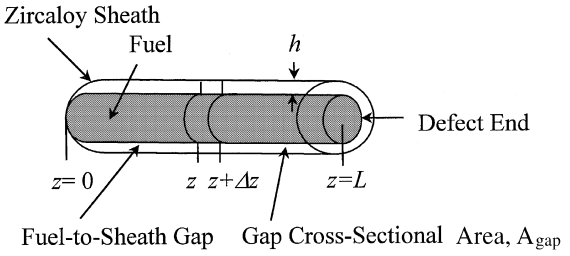

Fig. 1. Schematic of a defective fuel rod.

and y_i ($= c_i/c$) is the mole fraction of species i. The diffusivity parameter cD_{ij} (mol m^{-1} s^{-1}) corresponds to the i-jth pair of the binary mixture (see Appendix A).

For the present transport problem, in addition to the components of the bulk atmosphere (steam and hydrogen), there is also a release of fission gas from the fuel into the gap, which can be represented by xenon. Eq. (2) cannot be explicitly solved for the molar flux (N_i) for each species of the 3-component mixture because of the linear dependence of the resulting solution (i.e., the determinant is zero for this system of equations when it is cast in a matrix form). Consequently, for this ternary system (i.e., H_2O–H_2–Xe mixture), only two equations are independent due to the constraint on the mole fractions which must sum to unity

$$y_1 + y_2 + y_3 = 1. \tag{4}$$

Thus, Eq. (2) can be solved as a reduced system of two coupled equations (with $i = 1, 2$ and $n = 3$) for the molar fluxes N_1 and N_2, where employing Eq. (4) [18]

$$N_1 = -c\left(\mathscr{D}_{11} \frac{\partial y_1}{\partial z} + \mathscr{D}_{12} \frac{\partial y_2}{\partial z} \right) + y_1 N_T, \tag{5a}$$

$$N_2 = -c\left(\mathscr{D}_{21} \frac{\partial y_1}{\partial z} + {}_{22} \frac{\partial y_2}{\partial z} \right) + y_2 N_T. \tag{5b}$$

In the derivation of Eqs. (5a) and (5b), the total molar flux N_T is given by

$$N_T = N_1 + N_2 + N_3. \tag{6}$$

The multicomponent diffusion coefficients $\mathscr{D}_{ij}$ are defined as

$$\mathscr{D}_{11} = \frac{Y_{12} + Y_{32} + Y_{23}}{\det}, \quad \mathscr{D}_{12} = \frac{Y_{12} - Y_{13}}{\det}, \quad \mathscr{D}_{21} = \frac{Y_{21} - Y_{23}}{\det}, \quad \mathscr{D}_{22} = \frac{Y_{21} + Y_{31} + Y_{13}}{\det}, \tag{7}$$

where

$$\det = \frac{y_1}{D_{12}D_{13}} + \frac{y_2}{D_{12}D_{23}} + \frac{y_3}{D_{13}D_{23}} \tag{8}$$

and

$$Y_{12} = \frac{y_1}{D_{12}}, \quad Y_{13} = \frac{y_1}{D_{13}},$$

$$Y_{21} = \frac{y_2}{D_{12}}, \quad Y_{23} = \frac{y_2}{D_{23}}, \\ Y_{31} = \frac{y_3}{D_{13}}, \quad Y_{32} = \frac{y_3}{D_{23}}, \tag{9}$$

Thus, in general, for the 2-components ($i = 1$ and 2),

$$N_i = -c\left(\mathscr{D}_{i1}\frac{\partial y_1}{\partial z} + \mathscr{D}_{i2}\frac{\partial y_2}{\partial z}\right) + y_i N_T. \tag{10}$$

Finally, substituting Eq. (10) into Eq. (1) yields the one-dimensional transport equation (for species $i = 1$ and 2)

$$\frac{\partial(cy_i)}{\partial t} = \frac{\partial}{\partial z}\left[c\left(\mathscr{D}_{i1}\frac{\partial y_1}{\partial z} + \mathscr{D}_{i2}\frac{\partial y_2}{\partial z}\right) - y_i N_T\right] + q_i - r_i. \tag{11}$$

The corresponding system of equations for the stable fission gas (1≡Xe) and steam (2≡H_2O) is therefore given by

$$\frac{\partial(cy_1)}{\partial t} = \frac{\partial}{\partial z}\left[c\left(\mathscr{D}_{11}\frac{\partial y_1}{\partial z} + \mathscr{D}_{12}\frac{\partial y_2}{\partial z}\right) - y_1 N_T\right] + q_1(z,t), \tag{12a}$$

$$\frac{\partial(cy_2)}{\partial t} = \frac{\partial}{\partial z}\left[c\left(\mathscr{D}_{21}\frac{\partial y_1}{\partial z} + \mathscr{D}_{22}\frac{\partial y_2}{\partial z}\right) - y_2 N_T\right] - r_2^{\text{clad ox}}(z,t) - r_2^{\text{fuel ox}}(z,t). \tag{12b}$$

The hydrogen component (3≡H_2) follows directly from Eq. (4). In the derivation of Eq. (12a) there is no loss rate term since the xenon is chemically inert and stable. In addition, the source term is zero in Eq. (12b) since there are no chemical reactions which produce H_2O.The parameter q_1 in Eq. (12a) is equal to the stable fission gas release from the fuel matrix [18]

$$q_1 = \left(\frac{V}{S}\right)_{\text{fuel}} \frac{c_{\text{Xe}}^0}{h}\frac{\mathrm{d}f_{\text{rel}}}{\mathrm{d}t}, \tag{13}$$

where $(V/S)_{\text{fuel}}$ is the volume-to-surface ratio of the fuel ($= a_f/2$ where a_f is the fuel pellet radius) and h is the radial gap thickness. The parameter c_{Xe}^0 is the initial fission gas concentration in the fuel

$$c_{\text{Xe}}^0 = Y_{\text{Xe+Kr}} c_U \beta_f, \tag{14}$$

where $Y_{\text{Xe+Kr}}$ is the rare gas fission yield ($= 0.25$ atom fission^{-1}), c_U is the molar density of uranium in UO_2 ($= 41 \times 10^3$ mol m^{-3}), and β_f is the burnup fraction (i.e., 1 at.% burnup equals 0.95×10^4 MWd/tU). The fission gas release rate from the fuel ($\mathrm{d}f_{\text{rel}}/\mathrm{d}t$), which depends on the fuel-oxidation state, can be calculated by linking the present gap transport model to a mechanistic fission product release code (see Ref. [13]). Alternatively, assuming a constant release rate as a function of position in the gap, and neglecting any feedback effects due to fuel oxidation, this parameter can be estimated from the simple CORSOR-M correlation, such that [18,19]

$$\frac{\mathrm{d}f_{\text{rel}}}{\mathrm{d}t} = k_0 \exp(-Q_c/T)\,(1 - f_{\text{rel}}), \tag{15}$$

where $k_0 = 3.33 \times 10^3$ s^{-1} and $Q_c = 3.21 \times 10^4$ K. Eq. (15) requires an initial condition $f_{\text{rel}}(t=0) = f_{\text{rel}}^0$ where $t = 0$ is taken as the start of the transient. The loss terms for steam in Eq. (12b) (and the corresponding source terms for hydrogen), which result from the given oxidation process for the clad or fuel, are detailed in Section 2.4.

Finally, for the total gas balance in the gap, the conservation statement of Eq. (1) yields

$$\frac{\partial c}{\partial t} = -\frac{\partial N_T}{\partial z} + q_1. \tag{16}$$

This result follows where the production rate of hydrogen and the loss rate of steam are equal for a given chemical process (see Section 2.4) so that fission gas release is the only net source in the gap. It is also implicitly assumed that hydrogen losses do not occur in the gap, i.e., hydrogen absorption into the clad is prevented due to the production of a protective oxide layer on the inner clad surface as a result of the clad oxidation reaction.

The transport equations in Eqs. (12a) and (12b) can also be recast in a slightly different form using Eq. (16). In particular, multiplying Eq. (16) by y_i and using this relationship to account for the terms which arise from the chain rule for $\partial(cy_i)/\partial t$ and $\partial(y_i N_T)/\partial z$ in Eqs. (12a) and (12b), Eqs. (12a) and (12b) can be rewritten as [18]

$$c\frac{\partial y_1}{\partial t} = \frac{\partial}{\partial z}\left[c\left(\mathscr{D}_{11}\frac{\partial y_1}{\partial z} + \mathscr{D}_{12}\frac{\partial y_2}{\partial z}\right)\right] - N_T\frac{\partial y_1}{\partial z} + (1 - y_1)q_1(z,t), \tag{17a}$$

$$c\frac{\partial y_2}{\partial t} = \frac{\partial}{\partial z}\left[c\left(\mathscr{D}_{21}\frac{\partial y_1}{\partial z} + \mathscr{D}_{22}\frac{\partial y_2}{\partial z}\right)\right] - N_T\frac{\partial y_2}{\partial z} - y_2 q_1(z,t) - r_2^{\text{clad ox}}(z,t) - r_2^{\text{fuel ox}}(z,t). \tag{17b}$$

2.2. Solution methodology

2.2.1. General solution of Stefan–Maxwell equations

During a reactor transient, a temperature gradient may be present in the fuel rods, which should be known a priori based on reactor safety calculations. Thus, the temperature function $T(z,t)$ will be known for numerical solution of the gap transport equations. In addition, a pressure gradient may arise along the gap due to the continual release of stable fission gas into the gap [8–10]. The effect of the pressure gradient can be estimated as follows.

Assuming that the bulk velocity is the same as the mole average velocity, N_T can be estimated from the Hagen–Poiseuille flow law where, from a momentum balance, the bulk velocity (v) is calculated to be proportional to the pressure gradient ($\mathrm{d}P/\mathrm{d}z$), i.e., [8]

$$N_T = vc = \left[-\frac{h^2}{12\mu}\frac{\mathrm{d}P}{\mathrm{d}z}\right]c, \tag{18}$$

where h is the radial gap thickness and μ is the viscosity for a gas mixture (see Appendix B). Allowing for the possibility of a temperature gradient as well, the ideal gas law is given by

$$c(z,t) = \frac{P(z,t)}{RT(z,t)}, \tag{19}$$

where R is the ideal gas constant. Thus, Eqs. (16), (18) and (19) yield a partial differential equation for the pressure in the gap

$$\frac{1}{R}\frac{\partial(P/T)}{\partial t} = \frac{1}{12R}\frac{\partial}{\partial z}\left[\left(\frac{h^2}{\mu}\right)\left(\frac{\partial P}{\partial z}\right)\frac{P}{T}\right] + q_1. \tag{20}$$

This equation is subject to an initial and two boundary conditions:

$$P = P^0_{\text{sys}} = \text{constant}, \quad t = 0, \quad 0 < z < L, \tag{21a}$$

$$P = P_{\text{sys}}(t), \quad z = L, \quad t > 0, \tag{21b}$$

$$\mathrm{d}P/\mathrm{d}z = 0, \quad z = 0, \quad t > 0. \tag{21c}$$

where P^0_{sys} is the initial coolant pressure at $t = 0$ and $P_{\text{sys}}(t)$ is the bulk system pressure at the defect end of the rod (see Fig. 1). Eq. (21c) follows from Eq. (18) where it is assumed that the velocity $v = 0$ at the intact end of the rod. Thus, Eq. (20) can be numerically solved to provide $P(z,t)$.

As an illustrative example, Eq. (20) can also be solved analytically if steady-state flow conditions are achieved in relatively short period of time [8,10]. Thus, in the steady state, Eq. (16) becomes [8,10]

$$\frac{\mathrm{d}N_{\text{T}}}{\mathrm{d}z} = q_1. \tag{22}$$

Assuming a constant fission gas generation (q_1) along the gap, with no flow at the intact end of the rod (see Fig. 1), i.e., $N_{\text{T}} = 0$ at $z = 0$, the solution of Eq. (22) is

$$N_{\text{T}} = q_1 z. \tag{23}$$

Hence, from Eqs. (18), (19) and (23)

$$v(z) = -\frac{h^2}{12\mu}\frac{\mathrm{d}P}{\mathrm{d}z} = \frac{q_1 RTz}{P}. \tag{24}$$

Furthermore, assuming isothermal conditions and a constant radial gap, Eq. (24) can be directly integrated as

$$q_1 RT\int_x^L z\,\mathrm{d}z = -\frac{h^2}{12\mu}\int_{P(x)}^{P_{\text{sys}}} P\,\mathrm{d}P \tag{25}$$

yielding

$$P^2(z) = \frac{12q_1 RT\mu}{h^2}\left(L^2 - z^2\right) + P^2_{\text{sys}}. \tag{26}$$

If there is little gas release q_1, or a large radial gap h exists, $P(z) \approx P_{\text{sys}} = \text{constant}$, and therefore pressure gradient effects can be neglected. For instance, under realistic conditions, the pressure gradient is not expected to be significant since ballooning of the Zircaloy tubes is likely to occur at temperatures below 1000°C. Hence, the radial gap should be large (~1 mm), where an increased value of h will reduce the pressure gradient in accordance with Eq. (26). For example, employing Eq. (26) as shown in Ref. [8], for a CANDU-size rod with a length of 0.48 m and a small gap size of $h = 10$ μm, a pressure gradient of only $\Delta P = 0.055$ MPa was estimated along the entire length of the rod for a temperature transient at 1600 K (for an atmospheric system pressure of $P_{\text{sys}} = 0.1$ MPa). For larger gap thicknesses, the pressure gradient clearly becomes negligible (as predicted by Eq. (26)).

In fact, analogous equations to Eqs. (17a) and (17b) have been previously proposed for multi-component transport modelling for severe accident analysis in light water reactor fuel rods [18]. In this analysis, however, it was implicitly assumed that there was no pressure or temperature gradient in the gap, where the molar concentration c and temperature T were independent of z [18].

Thus, for a given transient temperature history along the rod, $T(z,t)$, and knowing $P(z,t)$ from Eq. (20) (or setting $P(z,t) = P_{\text{sys}}(t)$ if pressure gradient effects are negligible), the total molar concentration can be derived from Eq. (19). Given $c(z,t)$, Eq. (16) can then be solved for $N_{\text{T}}(z,t)$ employing the initial and boundary conditions

$$c = \frac{P^0_{\text{sys}}}{RT}, \quad t = 0, \quad 0 < z < L, \tag{27a}$$

$$N_{\text{T}} = 0, \quad z = 0, \quad t > 0, \tag{27b}$$

where P^0_{sys} is the initial coolant pressure at $t = 0$. The boundary condition in Eq. (27b) arises since there is no flow at the intact end of the rod. The distribution of the mole fractions for species 1 and 2 can then be determined by solving Eqs. (12a) and (12b) (or equivalently Eqs. (17a) and (17b)). The third species follows directly from Eq. (4). The initial and boundary conditions for Eqs. (12a) and (12b) are

$$y_1 = y^0_1, \quad y_2 = y^0_2, \quad \text{for } t = 0,\ 0 < z < L, \tag{28a}$$

$$\frac{\partial y_1}{\partial z} = \frac{\partial y_2}{\partial z} = 0, \quad \text{for } x = 0,\ t > 0, \tag{28b}$$

$$y_1 = 0, \quad y_2 = y^{\text{c}}_2(t), \quad \text{for } x = L,\ t > 0. \tag{28c}$$

The quantities y^0_1 and y^0_2 are the initial quantities specified for the given accident scenario at the start of the transient. The boundary conditions in Eq. (28b) follow from Eqs. (5a), (5b), (6) and (27b), and simply indicate that there is no flow at the intact end of the fuel rod (i.e., a reflexive condition). The boundary condition in Eq. (28c) indicates that the fission gas concentration is zero at the defect end since the fission gas is continually

being swept away by the bulk gas atmosphere flowing past the fuel rod. On the other hand, there is a constant supply of steam (with a mole fraction y_2^c) at this exposed end from the bulk atmosphere in the reactor coolant system (see Section 2.4.2.1).

The quantity of fission gas release q_1 into the gap will depend on the distribution of the molar fractions (due to the effect of the oxygen potential on the fuel oxidation and fission product solid-state diffusivity in the fuel matrix), and hence an iteration will be required in the solution of Eqs. (12a), (12b) and (20) when feedback effects are considered.

2.2.2. Approximate solution (diffusive-convective transport equation)

Alternatively, assuming that all of the species of the multi-component mixture have the same bulk flow $v(z)$, the present gap transport problem can also be recast into the form of a standard diffusive-convective transport equation where the Stefan–Maxwell equations can be used to yield an effective diffusivity [8,9]

For a flux resulting from both diffusion and a total molar bulk flow in a multi-component mixture [17]

$$N_i = -cD_{im}\nabla y_i + y_i\sum_{j=1}^{n} N_j, \tag{29}$$

where $N_j = c_j v_j$ and v_j is the velocity of species j (m s^{-1}). The parameter D_{im} is an "effective" binary diffusivity (m^2 s^{-1}) for the diffusion of species i in a mixture m. This quantity can be derived from the Stefan–Maxwell equations in Eq. (2). Hence, solving for ∇y_i in Eq. (29) and equating this to Eq. (2) gives

$$\frac{1}{cD_{im}} = \frac{\sum_{j=1}^{n}\left(1/cD_{ij}\right)\left(y_j N_i - y_i N_j\right)}{N_i - y_i\sum_{j=1}^{n} N_j}. \tag{30}$$

If $i=1$, Eq. (30) can therefore be written as

$$\frac{1}{cD_{1m}} = \frac{\sum_{j=1}^{n}\left(y_j/cD_{1j}\right)\left(v_1 - v_j\right)}{v_1 - \sum_{j=1}^{n} y_j v_j} = \frac{\sum_{j=2}^{n}\left(y_j/cD_{1j}\right)\left(v_1 - v_j\right)}{v_1 - y_1 v_1 - \sum_{j=2}^{n} y_j v_j}, \tag{31}$$

where the second relation follows since the numerator will equal zero when $j=1$. Now if the components $2, 3, \ldots n$ move with the same velocity, i.e., $v_2 = v_3 = \cdots = v_n = v$, Eq. (31) yields

$$\frac{1}{cD_{1m}} = \frac{\sum_{j=2}^{n}\left(y_j/cD_{1j}\right)\left(v_1 - v\right)}{v_1 - y_1 v_1 - v\sum_{j=2}^{n} y_j}. \tag{32}$$

No restrictions have been made on v_1 yet. Therefore in the limit that v_1 approaches v, and using the relation $\sum_{j=2}^{n} y_j = 1 - y_1$, one obtains

$$\frac{1}{cD_{1m}} = \lim_{v_1 \to v}\left[\frac{\sum_{j=2}^{n}\left(y_j/cD_{1j}\right)\left(v_1 - v\right)}{(1-y_1)(v_1 - v)}\right]. \tag{33}$$

Thus, applying l'Hopital's rule to evaluate the limit in Eq. (33) yields

$$\frac{1-y_1}{cD_{1m}} = \sum_{j=2}^{n}\left(\frac{y_j}{cD_{1j}}\right). \tag{34}$$

Hence, in the present case, if all components move with a bulk velocity $v(z)$

$$\frac{1-y_i}{cD_{im}} = \sum_{\substack{j=1 \\ j\neq i}}^{n}\left(\frac{y_j}{cD_{ij}}\right). \tag{35}$$

Finally, substituting Eq. (29) into Eq. (1), yields the one-dimensional diffusive-convective transport equation (compare with Eq. (11)).

$$\frac{\partial(cy_i)}{\partial t} = \frac{\partial}{\partial z}\left[cD_{im}\frac{\partial y_i}{\partial z} - y_i\sum_{j=1}^{n} N_j\right] + q_i - r_i. \tag{36}$$

In the particular case that all components move with the same velocity $v(z)$ so that

$$y_i\sum_{j=1}^{n} N_j = \frac{c_i}{c}\sum_{j=1}^{n} c_j v_j = c_i v(z),$$

Eq. (36) becomes

$$\frac{\partial(cy_i)}{\partial t} = \frac{\partial}{\partial z}\left[c\left(D_{im}\frac{\partial y_i}{\partial z} - y_i v(z)\right)\right] + q_i - r_i, \tag{37}$$

where cD_{im} is calculated from Eq. (35). The bulk flow velocity $v(z)$ follows from the Hagen–Poiseuille law in Eq. (24). Thus, using the ideal gas law in Eq. (19), Eq. (24) becomes

$$v(z) = -\frac{R}{12}\frac{\mathrm{d}}{\mathrm{d}z}\left(\frac{h^2 Tc}{\mu}\right), \tag{38}$$

where Eq. (38) generally assumes that the radial gap size and viscosity may also be a function of z.

Thus, using Eq. (37), the corresponding system of equations for the stable fission gas and steam is (compare with Eqs. (12a) and (12b)):

$$\frac{\partial(cy_1)}{\partial t} = \frac{\partial}{\partial z}\left[c\left(D_{1,m}\frac{\partial y_1}{\partial z} - y_1 v(z)\right)\right] + q_1(z,t), \tag{39a}$$

$$\frac{\partial(cy_2)}{\partial t} = \frac{\partial}{\partial z}\left[c\left(D_{2,m}\frac{\partial y_2}{\partial z} - y_2 v(z)\right)\right] - r_2^{\text{clad ox}}(z,t) - r_2^{\text{fuel ox}}(z,t). \tag{39b}$$

Analogous to Eq. (16), the total gas balance in the gap is

$$\frac{\partial c}{\partial t} = -\frac{\partial(cv(z))}{\partial z} + q_1. \tag{40}$$

Eq. (40) can be solved explicitly for $c(z,t)$ on substituting in the relation for $v(z)$ from Eq. (38), and solving the resultant second order partial differential equation with the following initial and boundary conditions (compare with Eqs. (27a) and (27b)):

$$c = \frac{P^0_{\text{sys}}}{RT}, \quad t = 0, \quad 0 < z < L, \tag{41a}$$

$$v(z) = 0 \Rightarrow \frac{\mathrm{d}c}{\mathrm{d}z} = -\left(\frac{c\mu}{h^2 T}\right)\frac{\mathrm{d}}{\mathrm{d}z}\left(\frac{h^2 T}{\mu}\right), \quad z = 0,$$

$$t > 0, \tag{41b}$$

$$c = \frac{P_{\text{sys}}(t)}{RT_{\text{sys}}(t)}, \quad z = L, \quad t > 0. \tag{41c}$$

The second relation in Eq. (41b) is a reflexive condition which follows directly from Eq. (38), where there is no flow at the intact end of the rod (Fig. 1). If h, T and μ are independent of z, Eq. (41b) reduces to the simple reflexive relation $\mathrm{d}c/\mathrm{d}z = 0$. At the defect end of the rod ($x = L$), the molar concentration is calculated from the bulk system pressure P_{sys} and temperature T_{sys}. Thus, with a knowledge of $c(z,t)$, $v(z)$ can be evaluated from Eq. (38). Finally, the mole fraction distributions then follow from Eqs. (39a), (39b) and (4). The former two equations are solved with the previous conditions detailed in Eqs. (28a)–(28c), where the effective diffusivity D_{im} is evaluated from Eq. (35) for each gas constituent i.

The present approximation slightly reduces the complexity of the governing transport equations (compare Eqs. (12a) and (12b) with Eqs. (39a) and (39b)), although with a numerical method of solution this approximation may not be worthwhile in terms of any significant computational savings.

2.3. Oxygen potential in the gap

Solving the given system of transport equations, one is able to obtain the oxygen potential along the gap as a function of time from the mole fraction (i.e., partial pressure) distribution. It is important to realize, however, that there is a feedback effect where the source term (q_1) in Eq. (13) actually depends on the state of fuel oxidation which, in turn, is affected by the oxygen potential [11–13]. Hence, the present model should be coupled to a mechanistic fission product release code to account for this effect.

The oxygen potential for an ideal gas mixture in the gap consisting of Xe, H_2O and H_2 can be evaluated as follows [13]. The total pressure P_{tot} (atm) is derived from the partial pressure P_j of each component j

$$P_{\text{tot}} = \sum_{j=1}^{n} P_j. \tag{42}$$

For the H_2O decomposition reaction

$$H_2O \overset{K_{H_2O}}{\Longleftrightarrow} H_2 + \frac{1}{2}O_2 \tag{43}$$

the equilibrium constant is

$$K_{H_2O} = \frac{P_{H_2}\sqrt{P_{O_2}}}{P_{H_2O}} = \exp\left\{0.9794\ \ln T - 1.1125 - \frac{28820}{T}\right\}. \tag{44}$$

If the H_2O dissociation required to maintain equilibrium is β, the partial pressures after dissociation are

$$P_{H_2O} = P^0_{H_2O} - \beta, \quad P_{H_2} = P^0_{H_2} + \beta, \quad P_{O_2} = \frac{\beta}{2}, \tag{45}$$

where the superscript 0 refers to the initial partial pressure quantities derived from the solution of the gap transport equations. Hence, the conditions for equilibrium can be described by combining Eqs. (42), (44) and (45),

$$K_{H_2O} = \frac{P^0_{H_2} + \beta}{P^0_{H_2O} - \beta} \times \sqrt{\frac{P_{\text{tot}}\left(\frac{1}{2}\beta\right)}{P^0_{H_2O} + P^0_{H_2} + P^0_{Xe} + \frac{1}{2}\beta}}. \tag{46}$$

Eq. (46) can be solved for β, and knowing the initial partial pressures, the partial pressures of the individual components, particularly that of the oxygen, can be determined from

$$\begin{aligned} \frac{P_{H_2}}{P_{\text{tot}}} &= \frac{P_{H^0_2+\beta}}{\sum_{j=1}^{n} P_j}, \quad \frac{P_{O_2}}{P_{\text{tot}}} = \frac{\frac{1}{2}\beta}{\sum_{j=1}^{n} P_j}, \\ \frac{P_{H_2O}}{P_{\text{tot}}} &= \frac{P^0_{H_2O} - \beta}{\sum_{j=1}^{n} P_j}, \quad \frac{P_{Xe}}{P_{\text{tot}}} = \frac{P^0_{Xe}}{\sum_{j=1}^{n} P_j}, \end{aligned} \tag{47}$$

where $\sum_{j=1}^{n} P_j = P^0_{H_2O} + P^0_{H_2} + P^0_{Xe} + 1/2\beta$. This methodology can also be used to calculate the oxygen partial pressure in the bulk coolant (see Section 2.4.2.1) where normally there is no inert gas constituent (i.e., $P^0_{Xe} = 0$).

2.4. Fuel rod oxidation processes

The production rate of hydrogen and the loss rate of steam are equal to one another for a given chemical process, i.e., $q^{\text{clad ox}}_{H_2} = r^{\text{clad ox}}_{H_2O}$ and $q^{\text{fuel ox}}_{H_2} = r^{\text{fuel ox}}_{H_2O}$. This result arises since the molar quantities of hydrogen and steam are balanced in each oxidation reaction for the Zircaloy and fuel:

$$Zr + 2H_2O \Longleftrightarrow ZrO_2 + 2H_2, \tag{48}$$

$$xH_2O + UO_2 \Longleftrightarrow UO_{2+x} + xH_2, \tag{49}$$

where x is the stoichiometry deviation in UO_{2+x}.

The kinetics for the fuel and Zircaloy oxidation processes are given in Sections 2.4.1 and 2.4.2, respectively. However, due to a reduced oxygen potential, as a result of hydrogen production during external clad oxidation (see Section 2.4.2), the internal fuel oxidation reaction does not typically become important until after the cladding has been completely oxidized. Water will also react more rapidly with the cladding than with the fuel [18]. In particular, equilibrium thermodynamics

indicate that the free energy of formation of the oxide is lower for ZrO_2 than for UO_{2+x} [12]. This result is demonstrated, for example, in annealing experiments with mini-elements containing loose-fitting end caps. Here, significant cesium release (indicating the occurrence of fuel oxidation) did not occur until after complete clad oxidation [11].

2.4.1. Urania oxidation

The fuel oxidation process has been extensively studied at atmospheric pressure where it has been shown that the kinetics are controlled by a reaction at the solid/gas interface. In this case, the fuel oxidation kinetics are described in Ref. [11]

$$c_U \left(\frac{V}{S}\right)_{\text{fuel}} \frac{dx}{dt} = c_U \alpha \{x_e - x(t)\}, \tag{50}$$

where c_U is the molar density of uranium (mol of uranium m^{-3}), α is a surface exchange coefficient ($=0.365 \exp\{-23500/T(K)\}$ m s^{-1}), x_e is the equilibrium stoichiometry deviation, and $(V/S)_{\text{fuel}}$ is the volume-to-surface area ratio of the fuel (m). Thus, using Eq. (50), the hydrogen production rate due to fuel oxidation is

$$q_{H_2}^{\text{fuel ox}} = c_U \left(\frac{V_{\text{fuel}}}{V_{\text{gap}}}\right) \frac{dx}{dt} = \frac{c_U \alpha}{h}(x_e - x(t)), \tag{51}$$

where V_{gap} is the gap volume (m^3) and h is the radial gap thickness (m).The value of x_e in Eq. (51) is obtained by equating the oxygen potential (i.e., oxygen partial pressure) in the fuel to that in the atmosphere (Section 2.3). The oxygen partial pressure in the fuel as a function of x, i.e., $P_{O_2}(x)$ (in atm), is given by either the Blackburn thermochemical model [20]

$$\ln P_{O_2} = 2\ln\left(\frac{x(2+x)}{1-x}\right) + 108x^2 - \frac{32\ 700}{T} + 9.92 \tag{52}$$

or the solid solution representation of Lindemer and Bessman [21]:

$$P_{O_2} = \min(P_1, P_2), \tag{53}$$

where P_1 and P_2 are given by

$$\begin{aligned} \ln P_1 &= 2\ln\left(\frac{x(1-2x)^2}{(1-3x)^3}\right) - \frac{37\ 621}{T} + 15.15, \\ \ln P_2 &= 4\ln\left(\frac{2x(1-2x)}{(1-4x)^2}\right) - \frac{43\ 298}{T} + 25.74. \end{aligned} \tag{54}$$

The fuel oxidation kinetics (dx/dt) in Eqs. (50) and (51) are only specifically valid at atmospheric pressure. However, for other system pressures (i.e., high pressure), these equations can be replaced with an expression derived from Langmuir adsorption theory [22–24]

$$c_U \left(\frac{V}{S}\right)_{\text{fuel}} \frac{dx}{dt} = n_s k'_a \frac{A(T)P_{H_2O}}{1 + A(T)P_{H_2O}} \left[1 - \frac{q(x)}{P_{H_2O}/P_{H_2}}\right], \tag{55}$$

where $n_s = 1.66 \times 10^{-6}$ mol m^{-2} is the density of adsorption sites (i.e., this value assumes a monolayer coverage of 10^{18} molecules m^{-2}), and P_{H_2O} and P_{H_2} are the partial pressures of steam and hydrogen (in atm). The parameter $A(T)$ (atm^{-1}) is defined as

$$A(T) = 1.0135 \times 10^5 \frac{s}{n_s k_a \sqrt{2\pi R T M_{H_2O}}}, \tag{56}$$

where s is the sticking probability $= 0.023$, T is the temperature (in K), $R = 8.314$ J mol^{-1} K^{-1} and $M_{H_2O} = 18 \times 10^{-3}$ kg mol^{-1}. Here $k'_a = 4.22 \times 10^{10} \exp\{-53810/(RT)\}$ s^{-1} is the steam dissociation rate constant which is determined from a fitting of the model to the available fuel oxidation data in Ref. [22]. The desorption rate constant, $k_a = 10^{13} \exp\{-40000/(RT)\}$ s^{-1}, follows for a typical chemisorption process. This type of adsorption is expected in light of the requirement for a strong adsorbate-substrate bond at high temperature. In addition, the assumption of a single monolayer coverage for n_s is reasonable considering that a monolayer is not normally exceeded with chemisorption. For these two rate constants, the ideal gas constant is given by $R = 1.987$ cal mol^{-1} K^{-1}. The oxygen activity $q(x)$ is derived from Eq. (44) where for a gas–solid equilibrium:

$$q(x) = \frac{\sqrt{P_{O_2}(x)}}{K_{H_2O}}. \tag{57}$$

Thus, for the calculation of the oxidation kinetics in Eq. (55), the steam-to-hydrogen partial pressure is derived from the solution of the transport equations in Section 2.2, and the $P_{O_2}(x)$ in Eq. (57) is evaluated from either Eq. (52) or Eq. (53).

Without existing data for high-pressure fuel oxidation, one cannot rule out the possibility of a Freundlich isotherm in the adsorption model [24]. In particular, the surface coverage term for Langmuir adsorption in Eq. (55), i.e.,

$$\theta = \frac{A(T)P_{H_2O}}{1 + A(T)P_{H_2O}} \tag{58}$$

can be replaced by the corresponding Freundlich isotherm

$$\theta = c_1 P_{H_2O}^{1/c_2}. \tag{59}$$

Therefore, as shown in Refs. [22,24], the parameter $(k'_a\theta)$ in Eq. (55) can be replaced using the Freundlich isotherm in Eq. (59)

$$k'_a\theta = 5.30 \times 10^8 \exp\left\{\frac{-21250}{T}\right\} \sqrt{P_{H_2O}}. \tag{60}$$

In fact, as expected, the activation energy in Eq. (60) (i.e., 21,250 K) is comparable to that of the surface exchange coefficient for the phenomenological model of Eq. (50) (i.e., 23,500 K). Both of the adsorption models are able to reasonably reproduce the observed oxidation kinetics over the lower pressure range of 0.01 to 1 atm

(from 1273 to 1700 K), where a roughly square-root dependence on the pressure is observed [11,24]. For example, over this temperature range at atmospheric pressure, the models are in agreement with one another within 17%; however, at higher pressure (e.g., 100 atm), the deviation is much greater. In particular, kinetic predictions with the Freundlich isotherm are a factor of ~3 times faster than that with the Langmuir isotherm, with a change in pressure from 1 to 100 atm at 1700 K. Experiments are required to confirm the high-pressure kinetics.

2.4.2. Zircaloy oxidation

Both internal (Section 2.4.2.1) and external (Section 2.4.2.2) oxidation of the Zircaloy cladding can occur depending on the steam availability. With a supply of steam to the outer clad surface, the Zircaloy oxidation process will be independent of the steam pressure since the rate-controlling process for this reaction is dictated by oxygen diffusion into the solid (i.e., oxide and metal), rather than by surface reaction as observed for the fuel oxidation process (see Section 2.4.1) [18,26,27]. The widely-used parabolic kinetic formulation provides a reasonable representation of the Zircaloy oxidation process under oxidizing conditions. However, if a strongly reducing atmosphere later becomes available, dissolution of the oxide scale into the remaining metal will occur which, in turn, can lead to absorption of hydrogen into the unprotected metal [26,27]. The parabolic scaling model cannot treat this behaviour and simply indicates that the oxide scale will remain in place. In addition, parabolic kinetics is only specifically applicable for a semi-infinite medium. For instance, for isothermal conditions, parabolic kinetics will match the proper moving-boundary diffusion solution until a small thickness of the clad is left, after which the diffusion model indicates an accelerated behaviour [28]. However, this effect is not significant since parabolic kinetics have been successfully applied in the analysis of hydrogen generation behaviour for steam experiments at the Oak Ridge National Laboratory and Chalk River Laboratories [25,29].

2.4.2.1. External clad oxidation and mass transfer effects. The mole fractions of the gas constituents in the bulk coolant at the defect site (e.g., the steam mole fraction $y_2^c(t)$ in Eq. (28c)) are boundary conditions which must be known a priori for a solution of the gap transport equations.

The mole fraction distributions in the coolant can be derived as follows. Consider a total molar gas flow rate Q (mol s^{-1}) into a control volume ($\Delta V_c = S_c\,\Delta z$) for the bulk coolant with a constant cross-sectional flow area S_c (m^2) (see Fig. 2). Similarly, applying the conservation statement of Eq. (1) to this volume element, the steam molar concentration in the bulk coolant $c^c_{H_2O}$ is given by

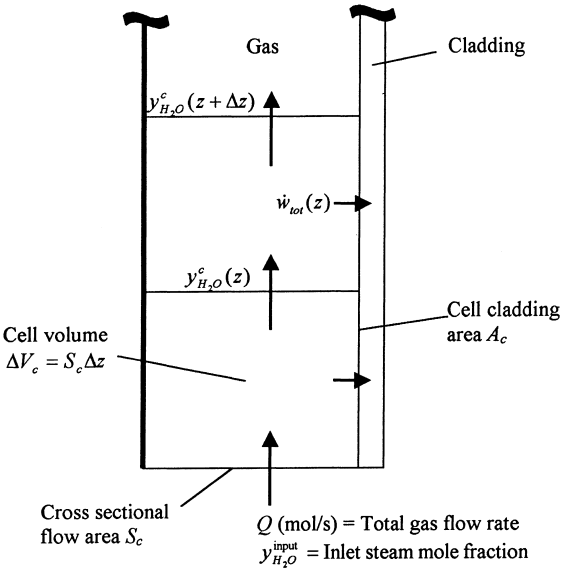

Fig. 2. Schematic of the cell geometry for the bulk coolant and cladding for the external cladding oxidation model.

$$\frac{\partial c^c_{H_2O}}{\partial t} = -\frac{\partial\left(\frac{Q}{S_c} y^c_{H_2O}\right)}{\partial z} - r^{\text{clad ox}}_{H_2O}, \tag{61}$$

where the term $r^{\text{clad ox}}_{H_2O}$ (mol m^{-3} s^{-1}) accounts for steam losses due to external clad oxidation. From the corrosion reaction in Eq. (48), since one mole of H_2O is consumed as one mole of H_2 is produced, the number of moles of gas is unchanged by the corrosion reaction if hydrogen absorption by the metal does not occur. In this case, Q will be independent of z so that Eq. (61) becomes

$$\frac{\partial\left(c^c y^c_{H_2O}\right)}{\partial t} = -\frac{Q}{S_c}\frac{\partial y^c_{H_2O}}{\partial z} - r^{\text{clad ox}}_{H_2O}. \tag{62}$$

Here c^c is the total molar gas concentration in the RCS such that (see Eq. (41c))

$$c^c = \frac{P_{sys}(t)}{RT_{sys}(t)} \tag{63}$$

and $r^{\text{clad ox}}_{H_2O}$ is given by

$$r^{\text{clad ox}}_{H_2O} = \left(\frac{\pi d}{S_c}\right)\dot{w}_{cor}, \tag{64}$$

where d is the fuel rod diameter (m). If w is the mass of zirconium consumed per unit area (kg m^{-2}) by the steam reaction, the reaction rate for steam is given by [25]

$$\dot{w}_{cor} = \frac{2}{M_{Zr}}\left(\frac{dw}{dt}\right), \tag{65}$$

where M_{Zr} is the molecular weight of zirconium ($=0.091$ kg mol^{-1}). The factor of two in Eq. (65) arises since one mole of Zr requires two moles of H_2O (see

Eq. (48)). From the parabolic rate law for Zircaloy corrosion

$$w^2 = k_w t \tag{66}$$

it follows that

$$\left(\frac{\mathrm{d}w}{\mathrm{d}t}\right) = \frac{1}{2}\sqrt{\frac{k_w}{t}}. \tag{67}$$

The parameter k_w (kg^2 m^{-4} s) is the parabolic rate constant:

$$k_w = k_{w0}\exp\left\{-\frac{Q_0}{RT}\right\}, \tag{68}$$

where k_{w0} and Q_0 are constants determined by various investigators (see Table 2).

For the numerical implementation of Eq. (66), for a given time step Δt, this equation can be discretized as [30]

$$\Delta w^2 = w^2(t+\Delta t) - w^2(t) = k_w \Delta t. \tag{69}$$

Thus, the time evolution of the Zircaloy mass consumption can be more accurately determined from the Taylor series expansion,

$$w(t+\Delta t) = w(t) + \frac{\mathrm{d}w}{\mathrm{d}t}\Delta t \tag{70}$$

by defining the derivative as [30]

$$\frac{\mathrm{d}w(t)}{\mathrm{d}t} = \frac{\sqrt{w^2(t)+k_w\Delta t} - w(t)}{\Delta t}. \tag{71}$$

Thus, neglecting any inert gas in the bulk coolant, the hydrogen and steam molar distributions in the RCS follows from the numerical solution of Eqs. (62)–(65), (70) and (71). Eq. (62) is subject to the following initial and boundary conditions:

$$y^{\mathrm{c}}_{\mathrm{H_2O}} = y^{0}_{\mathrm{H_2O}}, \quad t = 0, \quad 0 < z < L, \tag{72a}$$

$$y^{\mathrm{c}}_{\mathrm{H_2O}} = y^{\mathrm{input}}_{\mathrm{H_2O}}, \quad z = 0, \quad t > 0, \tag{72b}$$

where $y^{0}_{\mathrm{H_2O}}$ is the initial mole fraction for steam in the bulk coolant and $y^{\mathrm{input}}_{\mathrm{H_2O}}$ is the input mole fraction of steam in the bulk coolant at $z = 0$. The corresponding distribution for hydrogen is determined from the mass balance relation $y^{\mathrm{c}}_{\mathrm{H_2}} = 1 - y^{\mathrm{c}}_{\mathrm{H_2O}}$.

The present treatment implicitly assumes an unlimited supply of steam to the fuel rod. In particular, this analysis neglects any limitation as a result of mass transfer through the boundary layer. This latter effect can be included using the mass transfer rate law [26,27]

$$w_{\mathrm{MT}} = k_g y^{\mathrm{c}}_{\mathrm{H_2O}}. \tag{73}$$

The mass transfer coefficient k_{g} (mol m^{-2} s^{-1}) can be obtained from a heat-mass transfer analogy [12,13,17]

$$Nu_{ij} = \frac{k_{\mathrm{g}} D_{\mathrm{e}}}{cD_{ij}} \approx 4, \tag{74}$$

where Nu_{ij} is the Nusselt number for mass transfer (which equals 4 for laminar flow), D_{e} is the equivalent diameter (which equals the channel diameter minus the fuel rod diameter), and cD_{ij} is the diffusion coefficient parameter in Appendix A (which can be evaluated for the H_2O–H_2 binary mixture). Thus, in order to account for mass transfer effects, one simply replaces $\dot{w}_{\mathrm{cor}}$ in Eq. (64) by the more general relation [26,27]

$$\dot{w}_{\mathrm{tot}} = \min\left(\dot{w}_{\mathrm{cor}}, \dot{w}_{\mathrm{MT}}\right). \tag{75}$$

At steady state, $\partial\left(c^{\mathrm{c}} y^{\mathrm{c}}_{H_2O}\right)/\partial t = 0$, and Eq. (62) can be directly integrated over the cell distance Δz. Thus, if $r^{\mathrm{clad\ ox}}_{\mathrm{H_2O}}$ is constant over Δz (see Fig. 2),

$$\frac{Q}{S_{\mathrm{c}}}\int_{z}^{z+\mathrm{d}z} \mathrm{d}\left(y^{\mathrm{c}}_{\mathrm{H_2O}}\right) = -r^{\mathrm{clad\ ox}}_{\mathrm{H_2O}}\int_{z}^{z+\mathrm{d}z}\mathrm{d}z \tag{76a}$$

$$\Rightarrow y^{\mathrm{c}}_{\mathrm{H_2O}}(z+\mathrm{d}z) = y^{\mathrm{c}}_{\mathrm{H_2O}}(z) - \left(\frac{\Delta V_{\mathrm{c}}}{Q}\right) r^{\mathrm{clad\ ox}}_{\mathrm{H_2O}} = y^{\mathrm{c}}_{\mathrm{H_2O}}(z) - \left(\frac{A_{\mathrm{c}}}{Q}\right)\dot{w}_{\mathrm{tot}}, \tag{76b}$$

where A_{c} ($= \pi d\,\Delta z$) is the surface area of the clad in the given cell. The second relation in Eq. (76b) follows on use of Eqs. (64) and (75). This equation has also been proposed previously, where it was argued that the storage capacity of gas in the cell is much less than the total quantity of steam fed to the cell for the normal time duration $t_{\max}$ of a typical experiment or accident [27]. On multiplying Eq. (62) by ΔV_{c}, this condition is given by $c^{\mathrm{c}}\Delta V_{\mathrm{c}} \ll Q y^{\mathrm{input}}_{\mathrm{H_2O}} t_{\max}$. Therefore the term on the left-hand side of Eq. (62) can again be neglected, leading to the same result.

Thus, the steam distribution in the reactor coolant system can be given by the marching numerical solution of Eq. (76b) with the use of Eqs. (A.1), (65), (70), (71), (72a), (72b), (73), (74) and (75). An example of this calculation is given in Fig. 3 for an isothermal temper-

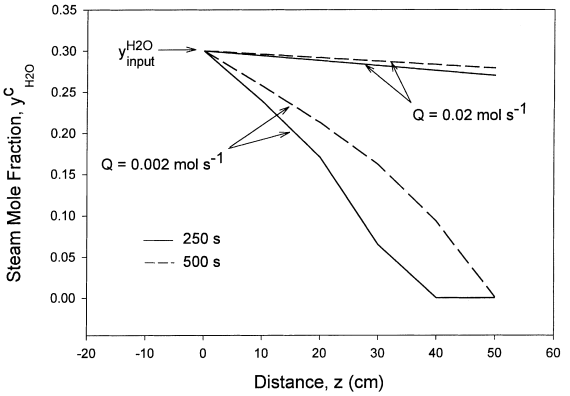

Fig. 3. Steam mole fraction distribution in the reactor coolant system due to external clad oxidation as a function of time and gas flow rate.

ature of 1730 K and an input steam mole fraction of $y_{H_2O}^{input} = 0.3$. The fuel rod dimensions are taken for a CANDU-type rod with a length and diameter of 50 and 1.3 cm, respectively, and a clad thickness of 0.43 mm. For the mass transfer calculation, a channel diameter of 2.5 cm is assumed, where the intermolecular parameters for hydrogen and steam are obtained from Table 1. The coefficients of Urbanic and Heidrick in Table 2 have been used for the parabolic kinetics. This simulation is performed with a step length $\Delta z = 1$ cm and a time step $\Delta t = 5$ s, and the results are given for a time of 250 and 500 s. As seen in Fig. 3, in the case of an essentially unlimited supply of steam (with a high gas flow rate of $Q = 2 \times 10^{-2}$ mol s^{-1}), the steam mole fraction distribution is approximately constant and equal to the input mole fraction. On the other hand, with a lower gas flow rate of $Q = 2 \times 10^{-3}$ mol s^{-1}, mass transfer effects become important where steam-starved conditions occur at the downstream end of the fuel rod so that only hydrogen is present.

2.4.2.2. Clad oxidation from the gap side. Analogously, the internal metal–water reaction will be mass transfer limited by the amount of steam which can be transported inside the thin gap. In this case

$$\dot{w}_{tot}^{inside} = \min(\dot{w}_{corr}, \dot{w}_{MT}^{inside}), \tag{77a}$$

and

$$\dot{w}_{MT}^{inside} = N_{H_2O} \frac{A_{gap}}{A_{Zr}}. \tag{77b}$$

Here, N_{H_2O} is the motor flux of steam given by Eq. (5b), A_{gap} is the gap cross-sectional area (Fig. 1) and A_{Zr}(m^2) is the internal surface of the clad. The reaction rate for $\dot{w}_{corr}$ for the Zircaloy is again given by Eqs. (65) and (67) (or equivalently Eqs. (70) and (71)). Thus the hydrogen production rate for the internal Zircaloy oxidation process can be similarly described by

$$q_{H_2}^{clad\ ox} = \dot{w}_{tot}^{inside} \frac{A_{Zr}}{V_{gap}} = \frac{\dot{w}_{tot}^{inside}}{h}, \tag{78}$$

where V_{gap} is the gap volume (m^3). The Zircaloy oxidation reaction will cease when the total clad thickness is consumed as a result of the single- or double-sided oxidation.

3. Concluding remarks

A model, based on a general Stefan–Maxwell formalism, has been developed to describe the multi-component transport of steam, hydrogen and fission gas in the fuel-to-clad gap of defective fuel rods during reactor accident conditions. The transport equations can be simplified somewhat in the case of a negligible pressure differential in the gap, i.e., this situation is expected with clad ballooning. The transport equations can also be recast into a diffusive–convective form with the assumption that the molar constituents in the gap have a common bulk flow. The calculation of the bulk flow from pressure differential in the gap is treated with a Hagen–Poiseuille flow law. With knowledge of the molar distributions, on solution of the transport equations, a methodology is given to calculate the oxygen potential along the gap as a function of time. The oxygen potential is an important parameter in severe accident analysis since it will dictate the low-volatile fission product and fuel vaporization behaviour, as well as the

Table 1
Intermolecular parameters for various gas constituents [a]

Gas component	Molecular weight, M (g mol^{-1})	Lennard-Jones parameters	
		σ (Å)	ε/κ (K)
H_2	2.016	2.915	38.0
He	4.003	2.576	10.2
H_2O	18.015	2.65	380
Xe	131.3	4.055	229

[a] Taken from Refs. [12,17].

Table 2
Parametric values for parabolic rate constant for Zircaloy oxidation in steam

Investigators	Temperature range (K)	k_{w0} (kg^2 m^{-4} s^{-1})	Q_0 ($\times 10^3$ J mol^{-1})
Baker and Just [31]	1273 to melting point	3.33×10^3	190
Urbanic and Heidrick [32]	1323–1853	2.96×10^1	140
	1853 to melting point	8.79×10^1	138
Pawel et al. [33]	1273–1773	2.94×10^2	167
Prater and Courtright [34]	1783–2773	2.68×10^4	220

(volatile) fission gas release kinetics. The gap can offer an important feedback effect, i.e., the outflowing fission gas can inhibit steam penetration into the gap which, in turn, will reduce the amount of fuel oxidation. Since an accelerated diffusion of fission gas results in oxidized fuel, a limiting effect on the release behaviour can be achieved, unlike the case for unclad (i.e., bare) fuel. In fact, a reduced cesium release has been observed in annealing experiments conducted in steam at the Chalk River Laboratories (CRL) with Zircaloy-clad specimens versus bare fuel fragments, even after the clad had been oxidized.

The production of hydrogen from the Zircaloy and fuel oxidation processes has been treated in the model. A model for fuel oxidation has been proposed for various pressure situations, based on Langmuir and Freundlich adsorption theory. Although both isotherms are able to reasonably predict the observed kinetics from 0.01 to 1 atm, no experimental data as yet are available to confirm the differing behaviour of the models at high pressure. The Zircaloy oxidation process is treated with parabolic kinetics. The possibility of rate limitation by gas-phase mass transfer of steam from the bulk coolant to the outer surface of the Zircaloy cladding has been considered. Simulation of the oxidation process at the outer clad surface is required to provide boundary conditions in the reactor coolant system for the gap transport problem. The simpler parabolic representation, however, is unable to account for oxide dissolution during reducing conditions; on the other hand, a more complex model based on moving-boundary diffusion theory could replace the parabolic treatment (as required). The present gap-transport model must be linked to a mechanistic code in order to account for the feedback effect of the fuel oxidation on the fission gas release.

The present model is currently being implemented and numerically solved using a finite difference method. In particular, this model is being solved for the specific conditions of the CRL annealing tests for interpretation of the fission product release behaviour. In addition, this analysis is examining the differences between the general and approximation representations of the Stefan–Maxwell treatment in Sections 2.2.1 and 2.2.2, and the effects of pressure and temperature gradients along the gap. More importantly, the feedback effect of fission gas release on the oxygen potential in the gap is being investigated.

Acknowledgements

The present analysis was supported by the Natural Sciences and Engineering Research Council of Canada. The author is very grateful to Professor D.R. Olander for many helpful discussions on the formulation and solution of the Stefan–Maxwell problem. The author would also like to thank Professor H.W. Bonin for a review of the manuscript.

Appendix A. Binary diffusion coefficient

The diffusivity parameter cD_{ij} (mol m^{-1} s^{-1}) ($=cD_{ji}$) for the i-jth pair of the binary mixture can be calculated from the standard kinetic theory of Chapman–Enskog [17]

$$cD_{ij} = 2.2646 \times 10^{-3} \frac{\sqrt{T(1/M_i + 1/M_j)}}{\sigma_{ij}^2 \Omega_{D_{ij}}}, \tag{A.1}$$

where T is the gas-mixture temperature (K), M_i is the molecular weight of gas component i (g mol^{-1}) and σ_{ij} is the collision diameter (Å). The collision integral $\Omega_{D_{ij}}$ is a function of the Lennard-Jones force constant ε_{ij}/κ (in K) [13]

$$\Omega_{D_{ij}} = \frac{1}{0.7049 + 0.2910 \ln(T\kappa/\varepsilon_{ij})}. \tag{A.2}$$

The combined quantities for the force constants can be evaluated as

$$\sigma_{ij} = \frac{\sigma_i + \sigma_j}{2}, \quad \frac{\varepsilon_{ij}}{\kappa} = \sqrt{\frac{\varepsilon_i}{\kappa}\frac{\varepsilon_j}{\kappa}}, \tag{A.3}$$

where the individual quantities for the gas components are given in Table 1.

Appendix B. Gas viscosity

For a gas mixture, the viscosity μ can be determined from [17]

$$\mu = \sum_{i=1}^{n} \frac{y_i \mu_i}{\sum_{j=1}^{n} y_j \phi_{ij}} \tag{B.1}$$

in which

$$\phi_{ij} = \frac{1}{\sqrt{8}} \left(1 + \frac{M_i}{M_j}\right)^{-1/2} \left[1 + \left(\frac{\mu_i}{\mu_j}\right)^{1/2} \left(\frac{M_j}{M_i}\right)^{1/4}\right]^2. \tag{B.2}$$

The individual viscosity μ_i (in g cm^{-1} s^{-1}) for each component can be calculated from

$$\mu_i = 2.6693 \times 10^{-5} \frac{\sqrt{M_i T}}{\sigma_i^2 \Omega_{\mu_i}}, \tag{B.3}$$

where T is in K, M_i is in g mol^{-1} and σ_i is in Å. The parameter $\Omega_{\mu i}$ can similarly be calculated from

$$\Omega_{\mu_i} = \frac{1}{0.6641 + 0.2581 \ln(T\kappa/\varepsilon_i)}. \tag{B.4}$$

References

[1] R. Beraha, G. Beuken, G. Frejaville, C. Leuthrot, Y. Musante, Nucl. Technol. 49 (1980) 426.
[2] B.J. Lewis, C.R. Phillips, M.J. Notley, Nucl. Technol. 73 (1986) 72.
[3] B.J. Lewis, F.C. Iglesias, D.S. Cox, E. Gheorghiu, Nucl. Technol. 92 (1990) 353.
[4] B.J. Lewis, J. Nucl. Mater. 175 (1990) 218.
[5] B.J. Lewis, R.D. MacDonald, N.V. Ivanoff, F.C. Iglesias, Nucl. Technol. 103 (1993) 220.
[6] H.W. Kalfsbeek, Nucl. Technol. 62 (1983) 7.
[7] B.J. Lewis, F.C. Iglesias, A.K. Postma, D.A. Steininger, J. Nucl. Mater. 244 (1997) 153.
[8] B.J. Lewis, H.W. Bonin, J. Nucl. Mater. 218 (1994) 42.
[9] Z.W. Lian, L.N. Carlucci, V.I. Arimescu, Convective-diffusive transport of fission products in the gap of a failed fuel element, in: Proceedings of the 15th Annual Conference of the Canadian Nuclear Society, Montreal, Que., June 5–8, 1994, Canadian Nuclear Society, 1994, Session 5C.
[10] M. Kinoshita, Evaluation of axial fission gas transport in power ramping experiments, in: IAEA Specialists' Meeting on Water Reactor Fuel Element Performance Computer Modelling, Bowness-on-Windermere, England, April 9–13, 1984.
[11] B.J. Lewis, B. André, B. Morel, P. Dehaudt, D. Maro, P.L. Purdy, D.S. Cox, F.C. Iglesias, M.F. Osborne, R.A. Lorenz, J. Nucl. Mater. 227 (1995) 83.
[12] B.J. Lewis, B. André, G. Ducros, D. Maro, Nucl. Technol. 116 (1996) 34.
[13] B.J. Lewis, B.J. Corse, W.T. Thompson, M.H. Kaye, F.C. Iglesias, P. Elder, R. Dickson, Z. Liu, J. Nucl. Mater. 252 (1998) 235.
[14] D.R. Olander, these Proceedings, p. 187.
[15] Z. Liu, P.H. Elder, R.S. Dickson, S.T. Craig, High-Temperature Fission-Product Release Measurement, unpublished.
[16] F.C. Iglesias, B.J. Lewis, P.J. Reid, P. Elder, these proceedings, p. 21.
[17] R.B. Bird, W.E. Stewart, E.N. Lightfoot, Transport Phenomena, Wiley, New York, 1960.
[18] D.R. Olander, Nucl. Eng. Des. 148 (1994) 273.
[19] M.R. Kuhlman, D.J. Lehmicke, R.O. Meyer, CORSOR User's Manual, NUREG/CR-4173, US Nuclear Regulatory Commission, March 1985.
[20] P.E. Blackburn, J. Nucl. Mater. 46 (1973) 244.
[21] T.B. Lindemer, T.M. Besmann, J. Nucl. Mater. 130 (1985) 473.
[22] B.V. Dobrov, V.V. Likhanskii, V.D. Orzin, A.A. Solodov, M.P. Kissane, H. Manenc, J. Nucl. Mater. 255 (1998) 59.
[23] D.R. Olander, J. Nucl. Mater. 252 (1998) 121.
[24] B.J. Lewis, unpublished.
[25] B.J. Lewis, D.S. Cox, F.C. Iglesias, J. Nucl. Mater. 207 (1993) 228.
[26] D.R. Olander, Nucl. Eng. Des. 148 (1994) 253.
[27] V. Mubayi, J.A. Gieseke, D.R. Olander, M. Schwarz, Victoria Independent Peer Review, Brookhaven National Laboratory Report, W-6436, April 1997.
[28] F.C. Iglesias, D.B. Duncan, S. Sagat, H.E. Sills, J. Nucl. Mater. 130 (1985) 36.
[29] T. Yamashita, Steam Oxidation of Zircaloy Cladding in the ORNL Fission Product Release Tests, NUREG/CR-4777 (ORNL/TM-10272), Oak Ridge National Laboratory, 1988.
[30] T.J. Heames, D.A. Williams, N.E. Bixler, A.J. Grimley, C.J. Wheatley, N.A. Johns, P. Domagala, L.W. Dickson, C.A. Alexander, I. Osborn-Lee, S. Zawadzki, J. Rest, A. Mason, R.Y. Lee, VICTORIA: A Mechanistic Model of Radionuclide Behaviour in the Reactor Coolant System Under Severe Accident Conditions, US Nuclear Regulatory Commission, NUREG/CR-5545, SAND90-0756, Rev. 1, R3, R4, December 1992.
[31] L. Baker, L.C. Just, Studies of Metal–Water Reaction at High Temperatures, part III, ANL-6548, 1962.
[32] V.F. Urbanic, T.R. Heidrick, J. Nucl. Mater. 75 (1978) 251.
[33] R.E. Pawel, J.V. Cathcart, R.A. McKee, J. Electrochem. Soc. 126 (1979) 1105.
[34] J.T. Prater, E.L. Courtright, Properties of Reactor Fuel Rod Materials at High Temperatures, Pacific Northwest Laboratory, NUREG/CR-4891, PNL-6164, 1987.